DOI: 10.1002/ejic.200700463

A New Approach to Novel Cluster Compounds of Lead(II) Phosphonates

Zi-Yi Du,[a] Hai-Bing Xu,[a] Xiu-Ling Li,[a] and Jiang-Gao Mao*[a]

Keywords: Lead / Sulfonate-phosphonates / Solvothermal synthesis / Cluster compounds

Five new lead(II) sulfonate-phosphonates, namely $[Pb_3(L)_2(H_2O)_2]\cdot 4H_2O$ (**1**), $[Pb(HL)(phen)]\cdot H_2O$ (**2**), $[Pb_6(L)_4(phen)_8]\cdot 3H_2O$ (**3**), $[Pb_6(L)_4(phen)_{10}]\cdot 2H_2O$ (**4**), and $[Pb_6(L)_4(4,4'\text{-bipy})(H_2O)_2]\cdot 2H_2O$ (**5**; H_3L = *m*-HO_3S-C_6H_4-PO_3H_2, phen = 1,10-phenanthroline, 4,4′-bipy = 4,4′-bipyridine) have been prepared and structurally characterized. Compound **1** features a novel 3D framework in which 1D chains of Pb_3O_4 cluster units are further bridged by sulfonate-phosphonate ligands, whereas compound **2** features a layer structure in which 1D chains of Pb_2O_4 clusters are further bridged by sulfonate-phosphonate ligands. Compounds **3** and **4** represent the first zero-dimensional lead(II) phosphonates and feature novel isolated hexanuclear lead(II) clusters in which six Pb^{II} ions are bridged by two tetradentate and two pentadentate phosphonate groups. Compound **5** features a 3D framework that is similar to that in compound **1** despite the different coordination modes for some sulfonate groups of the ligands. The main difference is that an aqua ligand in compound **1** is replaced by a nitrogen atom of the 4,4′-bipy ligand, which results in the splitting of the large cavities in compound **1** into two small apertures in compound **5**. Compounds **1** and **5** exhibit strong broad blue fluorescent emission bands at 398 and 420 nm, respectively.

Introduction

The chemistry of metal phosphonates has been expanding rapidly in recent years, mainly due to their potential application in the areas of catalysis, ion exchange, proton conductivity, intercalation chemistry, photochemistry, and material chemistry.[1] Similarly, the surface modification of inorganic surfaces with phosphonic acids is of growing importance since it opens the way to a large variety of novel functional materials.[1c,1d] Most investigations have been concentrated on the divalent transition and trivalent lanthanide elements.[2–6] Lead(II), however, has a lone pair of electrons and could therefore lead to interesting topological arrangements or to materials with redox as well as catalytic properties.[7–11] A wide variety of lead(II) phosphonates have been reported to date.[7–11] The strategy of using bisfunctional or multifunctional anionic units, such as diphosphonates, aminophosphonates, or phosphonocarboxylates, has led to a number of new lead phosphonates with microporous or open-framework structures.[7–10] Another useful way of building new types of phosphonate hybrids is by introducing a second metal linker, and we have used an acidic metal linker such as carboxylic acid or carboxylic-sulfonic acid to prepare a series of lead phosphonate hybrids with different architectures.[11] The carboxylic or carboxylic-sulfonic acid acts either as a multidentate bridging ligand or pendant group on the lead(II) phosphonate layer or intercalates between two layers.[11] These materials mostly exhibit layered structures, although 3D networks with micropores and 1D chains have also been reported.[7–11] Surprisingly, no discrete lead phosphonates have been reported thus far.

Three zinc(II) phosphonates based on tetranuclear or hexanuclear cluster units and four lanthanide(III) phosphonates based on tetranuclear cluster units have been isolated by our group by using *m*-sulfophenylphosphonic acid and a basic second metal linker such as 4,4′-bipy or phen.[12] The weak coordination ability of the sulfonate group and the bidentate chelating nature of the second ligand such as phen facilitate the formation of cage compounds with discrete cluster units. We therefore hoped that such an approach might be extended to the field of Pb^{II} phosphonates, where the isolation of cluster compounds is very difficult. The combination of Pb^{II} and *m*-sulfophenylphosphonic acid with a basic second metal linker led to five novel, discrete, 2D or 3D lead(II) sulfonate-phosphonates based on cluster units, namely $[Pb_3(L)_2(H_2O_2)]\cdot 4H_2O$ (**1**), $[Pb(HL)(phen)]\cdot H_2O$ (**2**), $[Pb_6(L)_4(phen)_8]\cdot 3H_2O$ (**3**), $[Pb_6(L)_4(phen)_{10}]\cdot 2H_2O$ (**4**), and $[Pb_6(L)_4(4,4'\text{-bipy})(H_2O)_2]\cdot 2H_2O$ (**5**). Herein we report their syntheses, crystal structures, and characterization.

Results and Discussion

Compounds **1**–**5** represent the first series of lead(II) compounds based on sulfonate-phosphonate ligands. Com-

[a] State Key Laboratory of Structural Chemistry, Fujian Institute of Research on the Structure of Matter, Chinese Academy of Sciences,
Fuzhou, Fujian 350002, P. R. China
E-mail: mjg@fjirsm.ac.cn

Supporting information for this article is available on the WWW under http://www.eurjic.org or from the author.

pounds **3** and **4** also represent the first discrete Pb^{II} polynuclear clusters based on phosphonate ligands. They exhibit novel, discrete, hexanuclear, 2D or 3D structures.

Synthesis

Compounds **1**–**5** were obtained during our systematic investigation of the Pb/L/phen (or bipy) systems with different Pb/L/phen ratios and pH values. We successfully prepared single-phase products for all five compounds except compound **4**. The preparations of compounds **1**–**5** rely on well-established hydrothermal methods. In general, a mixture of $Pb(OAc)_2$ and H_3L, with or without a second ligand such as phen or 4,4′-bipy, was treated hydrothermally for four days at 150 °C to produce crystalline products. The type of second ligand used has a strong influence on the final structure of these lead(II) sulfonate-phosphonates as compounds **2**–**5** were obtained instead of compound **1** when phen or 4,4′-bipy was employed as the second ligand. The molar ratio of reactants as well as the reaction pH also play important roles. Thus, compounds **2**–**4** were obtained from the $Pb(OAc)_2/H_3L$/phen system when the amount of phen and the reaction pH increased. We still do not fully understand why these compounds form under different reaction conditions, but it seems likely that the nature and amount of the second ligand play an important role by changing the coordination environment around the metal ions and the connectivities between the metal ions. Furthermore, the reaction medium becomes less acidic when more phen is used, and this can affect the coordination mode that the phosphonate ligand adopts.

Structure of $[Pb_3(L)_2(H_2O)_2]\cdot 4H_2O$ (1)

The structure of compound **1** features a novel porous 3D network with three unique lead(II) ions in the asymmetric unit (Figure 1). Pb(1) is six-coordinate with four phosphonate oxygen atoms from four L^{3-} anions as well as two sulfonate oxygen atoms from another two L^{3-} anions. Its coordination geometry can be described as a severely distorted PbO_6 octahedron. Pb(2) ion is five-coordinate with three phosphonate oxygen atoms from three L^{3-} anions and one sulfonate oxygen atom from another L^{3-} anion as well as an aqua ligand. The coordination geometry around Pb(2) can be described as a severely distorted ψ-PbO_5 octahedron with one site occupied by the lone pair of the Pb^{II} ion. The coordination environment of Pb(3) ion is similar to that of Pb(2) ion. The Pb–O distances [2.311(5)–2.833(7) Å] are similar to those reported for other lead(II) phosphonates and sulfonates.[7–11]

There are two unique L^{3-} ligands in compound **1**. The first, containing atoms P(1) and S(1), is hexadentate and bridges six lead(II) ions through its three phosphonate oxygen atoms and one sulfonate oxygen atom. Two phosphonate oxygen atoms [O(1) and O(3)] act as a μ^2-bridging ligand. The second sulfonate-phosphonate containing P(2) and S(2) is octadentate, with all three phosphonate oxygen atoms and three sulfonate oxygen atoms involved in metal coordination. Two phosphonate oxygen atoms [O(7) and O(8)] act as a μ^2-bridging ligand (Scheme 1).

The interconnection of the Pb^{II} ions via the bridging phosphonate groups leads to a 1D lead(II) phosphonate chain based on "Pb_3O_4" cluster units. Each pair of Pb^{II} ions within a Pb_3O_4 cluster unit is bridged by a pair of

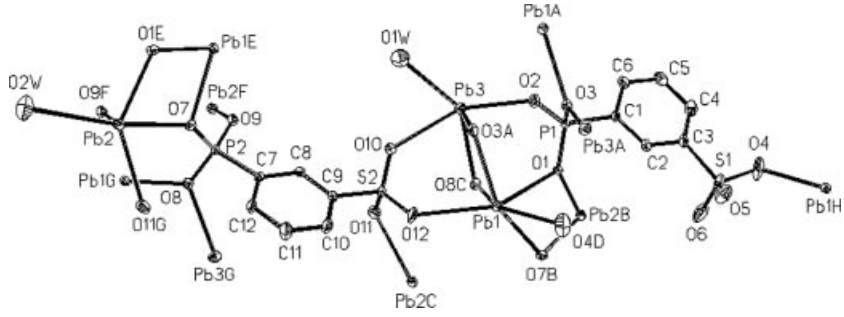

Figure 1. ORTEP representation of the selected unit of **1**. The thermal ellipsoids are drawn at 30% probability. Lattice water molecules have been omitted for clarity. Symmetry codes for the generated atoms: A) 1 – *x*, 1 – *y*, 1 – *z*; B) 1/2 + *x*, 1/2 – *y*, 1/2 + *z*; C) 3/2 – *x*, 1/2 + *y*, 1/2 – *z*; D) 3/2 – *x*, –1/2 + *y*, 3/2 – *z*; E) 1/2 + *x*, 1/2 – *y*, 3/2 – *z*; F) 1 – *x*, –*y*, –*z*; G) 3/2 – *x*, –1/2 + *y*, 1/2 – *z*; H) 3/2 – *x*, 1/2 + *y*, 3/2 – *z*.

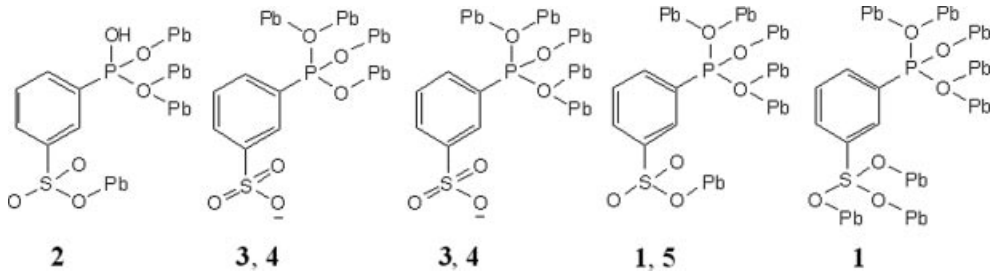

Scheme 1. The coordination modes of *m*-sulfophenylphosphonic acid in compounds **1**–**5**.

phosphonate oxygen atoms, and neighboring cluster units are further interconnected by bridging phosphonate and sulfonate groups into a 1D hybrid chain (Figure 2, a). These 1D chains are further cross-linked by the bridging L^{3-} ligands into a 3D network with long, narrow apertures along *a*-axis (Figure 3). The total solvent accessible space is about 24.3% of the cell volume according to our calculations.[13] The lattice water molecules are located in the above apertures and there are a number of hydrogen bonds between sulfonate oxygen atom O(11), the aqua ligands, and lattice water molecules (Table 1), with O···O contacts ranging from 2.71(1) to 3.03(1) Å. It is interesting to note that the hydrogen bonds between water molecules lead to the formation of a 1D water chain along the *a*-axis (Figure 2, b).

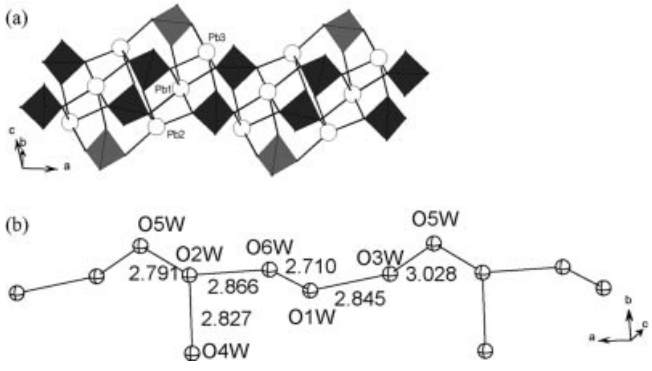

Figure 2. A 1D lead sulfonate-phosphonate chain based on Pb_3O_4 cluster units (a) and a 1D hydrogen-bonded water chain (b) in compound **1**. The CPO_3 and CSO_3 groups are shaded in dark and medium gray, respectively. Pb, O, and C atoms are drawn as white, crossed and black circles, respectively.

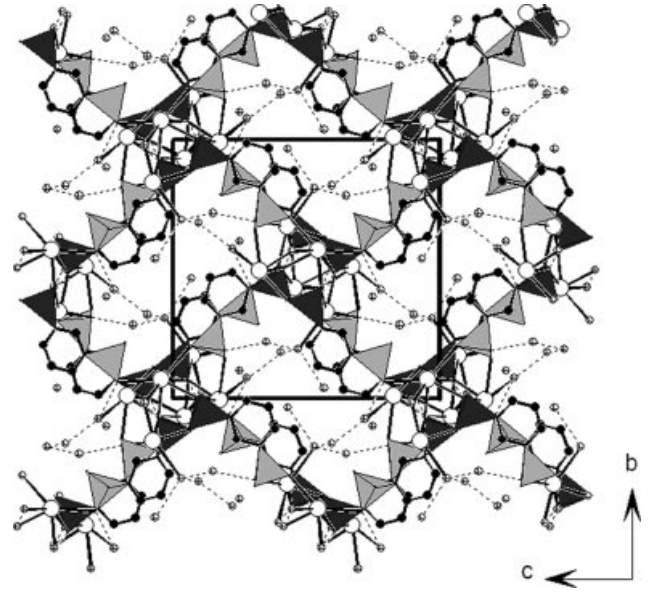

Figure 3. View of the structure of compound **1** along the *a*-axis. The CPO_3 and CSO_3 groups are shaded in dark and medium grey, respectively. Pb, O, and C atoms are drawn as open, crossed and black circles, respectively. Hydrogen bonds are drawn as dashed lines.

Table 1. Selected bond lengths [Å] for compounds **1**–**5**.[a]

1			
Pb(1)–O(8)#1	2.440(4)	Pb(1)–O(1)	2.486(4)
Pb(1)–O(3)#2	2.556(5)	Pb(1)–O(7)#3	2.584(4)
Pb(1)–O(12)	2.723(5)	Pb(1)–O(4)#4	2.781(6)
Pb(2)–O(9)#5	2.362(4)	Pb(2)–O(7)	2.370(4)
Pb(2)–O(1)#6	2.528(4)	Pb(2)–O(11)#7	2.659(5)
Pb(2)–O(2W)	2.833(7)	Pb(3)–O(3)#2	2.311(5)
Pb(3)–O(2)	2.445(5)	Pb(3)–O(8)#1	2.592(4)
Pb(3)–O(1W)	2.634(7)	Pb(3)–O(10)	2.797(5)
Hydrogen bonds			
O(11)···O(5W)	2.764(8)	O(1W)···O(6W)	2.71(1)
O(1W)···O(3W)	2.85(1)	O(2W)···O(5W)#5	2.79(1)
O(2W)···O(4W)#5	2.83(1)	O(2W)···O(6W)#5	2.87(1)
O(3W)···O(5W)#8	3.03(1)		
2			
Pb(1)–N(2)	2.446(6)	Pb(1)–N(1)	2.499(5)
Pb(1)–O(2)#1	2.531(5)	Pb(1)–O(1)#2	2.550(5)
Pb(1)–O(1)	2.727(5)	Pb(1)–O(5)#3	2.820(5)
P(1)–O(2)	1.496(5)	P(1)–O(1)	1.512(5)
P(1)–O(3)	1.579(5)		
Hydrogen bonds			
O(3)···O(4)#4	2.650(8)	O(1W)···O(2)#1	2.848(8)
3			
Pb(1)–O(3)	2.320(6)	Pb(1)–O(8)#1	2.353(5)
Pb(1)–N(2)	2.544(7)	Pb(1)–N(1)	2.595(7)
Pb(2)–O(7)	2.291(5)	Pb(2)–O(2)#1	2.468(5)
Pb(2)–O(7)#1	2.657(5)	Pb(2)–N(6)	2.669(6)
Pb(2)–O(1)	2.697(5)	Pb(2)–N(5)	2.766(7)
Pb(3)–O(9)#1	2.463(7)	Pb(3)–O(1)	2.482(6)
Pb(3)–O(3)	2.614(8)	Pb(3)–N(4)	2.66(1)
Pb(3)–N(3)	2.73(1)	Pb(3)–N(7)	2.84(1)
Pb(3)–N(8)	3.00(1)		
Hydrogen bonds			
O(6)···O(2W)	2.78(3)		
4			
Pb(1)–O(8)#1	2.386(6)	Pb(1)–O(1)	2.494(6)
Pb(1)–N(8)	2.502(8)	Pb(1)–N(7)	2.697(9)
Pb(1)–N(10)	2.853(8)	Pb(1)–N(9)	2.95(1)
Pb(2)–O(7)	2.294(5)	Pb(2)–O(2)#1	2.431(6)
Pb(2)–N(2)	2.614(8)	Pb(2)–O(3)	2.625(5)
Pb(2)–N(1)	2.708(8)	Pb(2)–O(7)#1	2.750(5)
Pb(3)–O(9)#1	2.286(6)	Pb(3)–O(1)	2.572(6)
Pb(3)–O(3)	2.597(5)	Pb(3)–N(6)	2.778(8)
Pb(3)–N(5)	2.814(9)	Pb(3)–N(3)	2.821(8)
Pb(3)–N(4)	2.880(8)		
Hydrogen bonds			
O(12)···O(1W)	3.04(1)		
5			
Pb(1)–O(1)	2.367(6)	Pb(1)–O(12)#1	2.475(6)
Pb(1)–O(11)#2	2.535(6)	Pb(1)–O(3)#3	2.597(6)
Pb(1)–O(5)#4	2.882(9)	Pb(2)–O(10)#1	2.283(6)
Pb(2)–O(11)#2	2.441(6)	Pb(2)–O(8)	2.531(7)
Pb(2)–N(1)	2.631(9)	Pb(2)–O(1)	2.713(6)
Pb(3)–O(3)#3	2.270(6)	Pb(3)–O(2)	2.334(6)
Pb(3)–O(12)#1	2.496(6)	Pb(3)–O(1W)	2.81(1)
Hydrogen bonds			
O(7)···O(2W)	2.90(1)	O(9)···O(1W)#5	2.93(1)
O(1W)···O(2W)#3	2.84(2)		

[a] Symmetry codes: for **1**: #1 $-x + 3/2$, $y + 1/2$, $-z + 1/2$; #2 $-x + 1$, $-y + 1$, $-z + 1$; #3 $x + 1/2$, $-y + 1/2$, $z + 1/2$; #4 $-x + 3/2$, $y - 1/2$, $-z + 3/2$; #5 $-x + 1$, $-y$, $-z$; #6 $x - 1/2$, $-y + 1/2$, $z - 1/2$; #7 $-x + 3/2$, $y - 1/2$, $-z + 1/2$; #8 $x - 1$, y, z. For **2**: #1 $-x + 1$, $-y + 2$, $-z + 2$; #2 $-x$, $-y + 2$, $-z + 2$; #3 x, $y - 1$, z; #4 $-x$, $3 - y$, $2 - z$. For **3**: #1 $-x + 1$, $-y + 1$, $-z + 1$. For **4**: #1 $-x + 1$, $-y$, $-z + 1$. For **5**: #1 $x - 1/2$, $-y - 1/2$, $z - 1/2$; #2 $-x - 3/2$, $y - 1/2$, $-z + 1/2$; #3 $-x - 3$, $-y - 1$, $-z$; #4 $-x - 5/2$, $y - 1/2$, $-z + 1/2$; #5 $-x - 2$, $-y - 1$, $-z$.

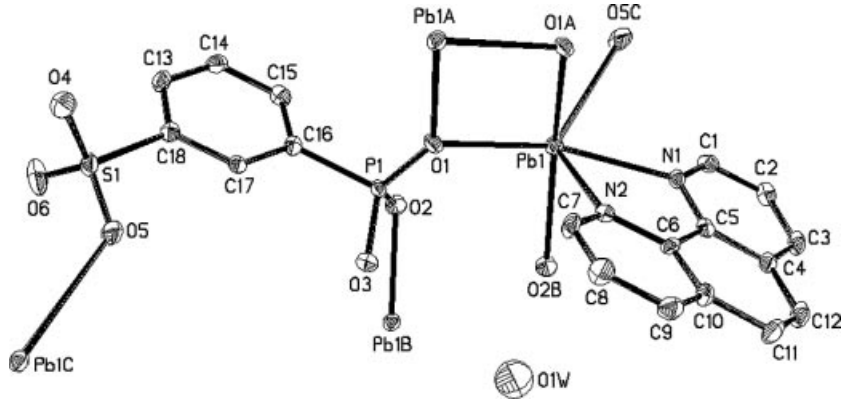

Figure 4. ORTEP representation of the selected unit of **2**. The thermal ellipsoids are drawn at 30% probability. Symmetry codes for the generated atoms: A) $-x$, $2-y$, $2-z$; B) $1-x$, $2-y$, $2-z$; C) x, $-1+y$, z.

The open framework of compound **1** remains intact after heating at 180 °C for 3 h based on X-ray powder diffraction studies (see Supporting Information).

Structure of $[Pb(HL)(phen)]\cdot H_2O$ (2)

The structure of compound **2** features a layered architecture. The Pb(1) ion is six-coordinate with three phosphonate oxygen atoms from three HL^{2-} anions, one sulfonate oxygen atom from another HL^{2-} anion, and one bidentate chelating phen ligand (Figure 4). The coordination geometry around Pb(1) can be described as a severely distorted PbO_4N_2 octahedron, with Pb–O [2.531(5)–2.820(5) Å] and Pb–N [2.446(6)–2.499(5) Å] distances similar to those reported for other lead(II) phosphonates and sulfonates.[7–11]

There is one unique HL^{2-} ligand in compound **2**. The phosphonate group of this ligand is singly protonated, as indicated by the much longer P(1)–O(3) bond [1.579(5) Å] than those of the other two P–O bonds [P(1)–O(2) 1.496(5), P(1)–O(1) 1.512(5) Å]. The HL^{2-} ligand is tetradentate and bridges four lead(II) ions via its two phosphonate oxygen atoms and one sulfonate oxygen atom (Scheme 1). O(1) acts as a μ^2-metal linker. Each pair of Pb^{II} ions is bridged by a pair of phosphonate oxygen atoms into a Pb_2O_2 dimer. These Pb_2O_2 dimeric units are further interconnected by bridging phosphonate groups into a 1D chain along the *a* axis, and these chains are further connected by the bridging HL^{2-} ligands into a layered structure (Figure 5). Strong hydrogen bonds are formed between noncoordinated phosphonate and sulfonate oxygen atoms [O(3)···O(4) 2.650(8) Å; symmetry code: $-x$, $3-y$, $2-z$) within the 2D layer. The 2D layers in compound **2** are assembled into a three dimensional structure through van der Waals forces (Figure 6). The lattice water molecules are located at the cavities of the structure and are involved in hydrogen bonding with coordinated phosphonate oxygen atom O(2) (Table 1).

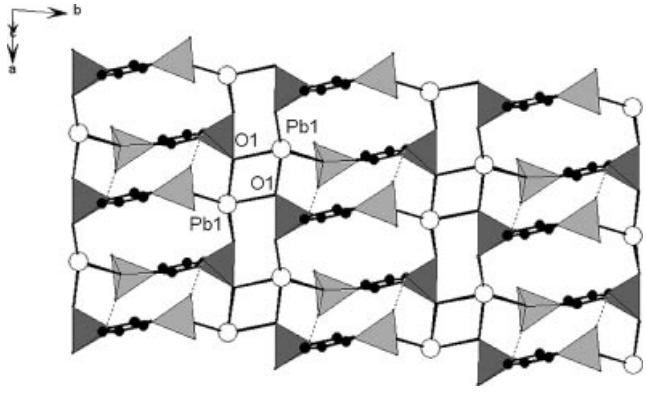

Figure 5. A lead(II) sulfonate-phosphonate layer in compound **2**. The CPO_3 and CSO_3 groups are shaded in medium and light grey, respectively. The phen ligands have been omitted for clarity. Hydrogen bonds are drawn as dashed lines.

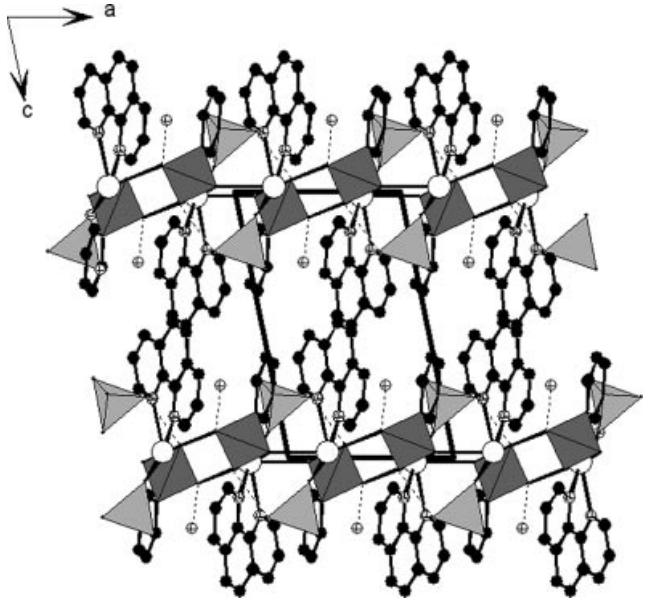

Figure 6. View of the structure of compound **2** down the *a*-axis. The CPO_3 and CSO_3 groups are shaded in medium and light gray, respectively. Pb, O, N and C atoms are drawn as open, crossed, octanded, and black circles, respectively. Hydrogen bonds are drawn as dashed lines.

Structure of $[Pb_6(L)_4(phen)_8]\cdot 3H_2O$ (3)

The structure of compound **3** features an isolated hexanuclear lead(II) cluster unit. There are three crystallographically independent lead(II) ions in the structure (Figure 7). The Pb(1) ion is four-coordinate with two phosphonate oxygen atoms from two L^{3-} anions as well as one bidentate chelating phen ligand. The coordination geometry around Pb(1) can best be described as a slightly distorted ψ-PbO_4 square-pyramid. The Pb(2) ion is six-coordinate with four phosphonate oxygen atoms from four L^{3-} anions as well as one bidentate chelating phen ligand. The coordination geometry around Pb(2) can be described as a slightly distorted ψ-PbO_4N_2 pentagonal pyramid with the lone pair occupying the open site of the pyramid. Pb(3) is seven-coordinate with three phosphonate oxygen atoms from two L^{3-} anions as well as two bidentate chelating phen ligands. The coordination geometry around Pb(3) can best be described as an irregular PbO_4N_2 polyhedron. The Pb–O [2.291(5)–2.697(5) Å] and Pb–N [2.544(7)–3.00(1) Å] distances are similar to those reported for other lead(II) phosphonates and sulfonates.[7–11]

There are two unique L^{3-} anions in compound **3**. The first, which contains P(1) and S(1), is pentadentate and bridges four Pb^{II} ions by using its three phosphonate oxygen atoms, whereas the other L^{3-} anion, which contains P(2) and S(2), is tetradentate and bridges four Pb^{II} ions through its three phosphonate oxygen atoms. O(1), O(3), and O(7) act as a μ^2-bridging ligand (Figure 7, Scheme 1). The interconnection of six Pb^{II} ions by the above two types of L^{3-} anions results in a novel hexanuclear cluster unit (Figure 8, a) which can be viewed as a double-cage structure. This "double-cage" hexanuclear cluster unit is different from our previously reported "chair-like" hexanuclear cluster units in zinc(II) sulfonate-phosphonates[8] owing to the different coordination modes of the sulfonate-phosphonate ligands. Thus, the two independent L^{3-} ligands in $[Zn_6L_4(phen)_8]\cdot 11H_2O$ connect three and four Zn^{II} ions, respectively, whereas each L^{3-} ligand in $[Zn_6L_4(bipy)_6(H_2O)_4]\cdot 18H_2O$ bridges three Zn^{II} ions.

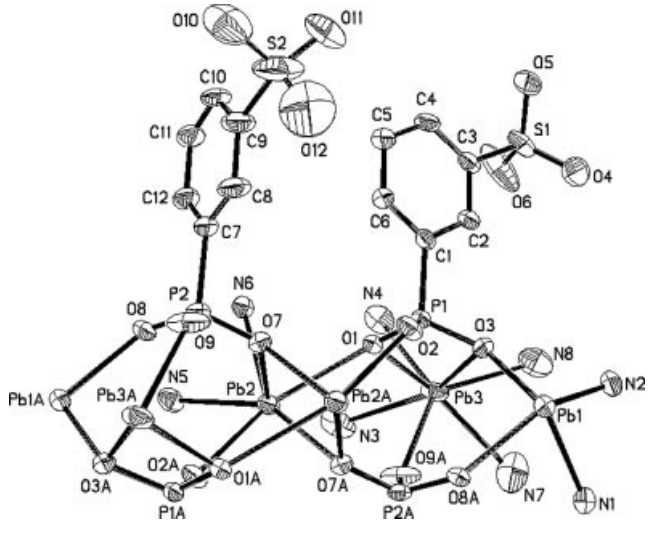

Figure 7. ORTEP representation of the selected unit of **3**. The thermal ellipsoids are drawn at 30% probability. Lattice water molecules and the carbon atoms of the phen ligands have been omitted for clarity. Only one orientation is shown for the disordered Pb(3) atom for the sake of clarity. Symmetry codes for the generated atoms: A) $1-x$, $1-y$, $1-z$.

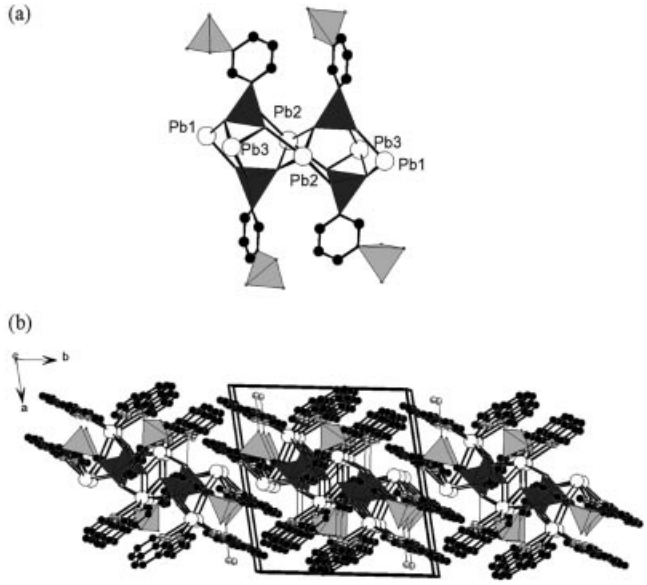

Figure 8. A $\{Pb_6L_4\}$ cluster unit in compound **3** (a) and a view of the structure of compound **3** down the *c*-axis (b). The CPO_3 and CSO_3 groups are shaded in dark and light gray, respectively. Pb, O, N and C atoms are drawn as open, crossed, octanded, and black circles, respectively. Hydrogen bonds are drawn as dashed lines.

The discrete clusters in compound **3** are assembled into a three dimensional structure through van der Waals forces (Figure 8, b). The lattice water molecules are located in the cavities of the structure, and O(2w) forms a hydrogen bond with the noncoordinating sulfonate oxygen atom O(6) (Table 1).

Structure of $[Pb_6(L)_4(phen)_{10}]\cdot 2H_2O$ (4)

Compound **4** contains two more phen ligands than compound **3**. Its structure also features an isolated hexanuclear Pb^{II} cluster similar to that in compound **3**. There are three crystallographically independent lead(II) ions in the asymmetric unit (Figure 9). Pb(1) is six-coordinate with two phosphonate oxygen atoms from two L^{3-} anions as well as two bidentate chelating phen ligands. The coordination geometry around Pb(1) can be described as a distorted ψ-PbO_2N_4 pentagonal pyramid. Pb(2) is six-coordinate with four phosphonate oxygen atoms from four L^{3-} anions as well as a bidentate chelating phen ligand. Pb(3) is seven-coordinate with three phosphonate oxygen atoms from two L^{3-} anions as well as two bidentate chelating phen ligands. The coordination environments around Pb(2) and Pb(3) are same as those in compound **3**. The Pb–O [2.286(6)–2.750(5) Å] and Pb–N [2.502(8)–2.95(1) Å] distances are similar to those reported for other lead(II) phosphonates and sulfonates.[7–11]

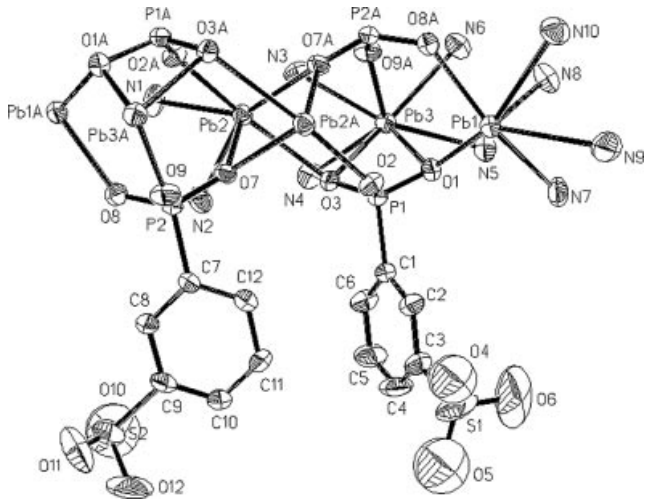

Figure 9. ORTEP representation of the selected unit of **4**. The thermal ellipsoids are drawn at 30% probability. Lattice water molecules and carbon atoms of the phen ligands have been omitted for clarity. Only one orientation is shown for the disordered O(11) atom for the sake of clarity. Symmetry codes for the generated atoms: A) $1 - x, -y, 1 - z$.

The coordination modes of the two unique L^{3-} anions in compound **4** are the same as those in compound **3** which means that the cluster unit of compound **4** is similar to that of compound **3**, the only difference being that Pb(1) in compound **4** has a higher coordination number due to the coordination of an additional phen ligand.

The discrete clusters in compound **4** are also assembled into a three-dimensional structure through van der Waals forces as well as a π···π packing interaction between the phen ligands (Figure 10). The lattice water molecules [O(1w)] are located in the cavities and form weak hydrogen bonds with the noncoordinating sulfonate oxygen atoms O(12) (Table 1).

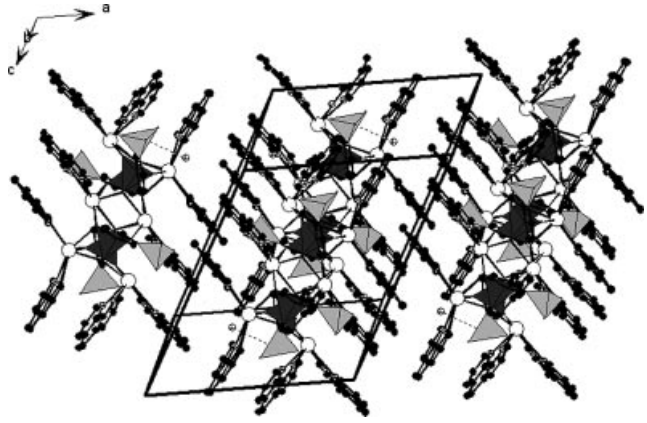

Figure 10. View of the structure of compound **4** down the *b*-axis. The CPO_3 and CSO_3 groups are shaded in dark and light gray, respectively. Pb, O, N, and C atoms are drawn as open, crossed, octanded, and black circles, respectively. Hydrogen bonds are drawn as dashed lines.

Structure of $[Pb_6(L)_4(4,4'\text{-bipy})(H_2O)_2]\cdot 2H_2O$ (5)

The structure of compound **5** features a complex 3D network. There are three unique Pb^{II} ions in the asymmetric unit of compound **5** (Figure 11). Pb(1) is five-coordinate with four phosphonate oxygen atoms from four L^{3-} anions and one sulfonate oxygen atom from another L^{3-} anion. The coordination geometry around Pb(1) can be described as a distorted ψ-PbO_5 octahedron with one axial site occupied by the lone pair of the Pb^{II} ion. Pb(2) is five-coordinate with three phosphonate oxygen atoms from three L^{3-} anions, one sulfonate oxygen atom from another L^{3-} anion, and a nitrogen atom from a 4,4′-bipy ligand. The coordination geometry around Pb(2) can be described as a severely distorted ψ-PbO_4N octahedron with one site occupied by the lone pair of the Pb^{II} ion. Pb(3) is four-coordinate with three phosphonate oxygen atoms from three L^{3-} anions and one aqua ligand. The coordination geometry around Pb(3) can be described as a distorted ψ-PbO_4 trigonal bipyramid with one pyramidal site occupied by the lone pair of the Pb^{II} ion. The Pb–O [2.270(6)–2.882(9) Å] and Pb–N [2.631(9) Å] distances are similar to those reported for other lead(II) phosphonates and sulfonates.[7–11]

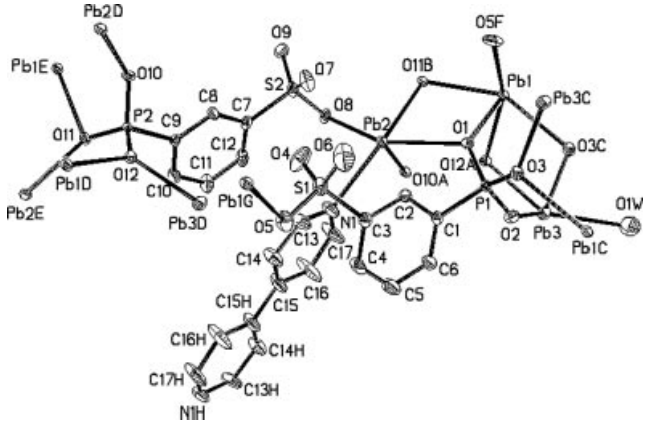

Figure 11. ORTEP representation of the selected unit of **5**. The thermal ellipsoids are drawn at 30% probability. Lattice water molecules have been omitted for clarity. Symmetry codes for the generated atoms: A) $-1/2 + x, -1/2 - y, -1/2 + z$; B) $-3/2 - x, -1/2 + y, 1/2 - z$; C) $-3 - x, -1 - y, -z$; D) $1/2 + x, -1/2 - y, 1/2 + z$; E) $-3/2 - x, 1/2 + y, 1/2 - z$; F) $-5/2 - x, -1/2 + y, 1/2 - z$; G) $-5/2 - x, 1/2 + y, 1/2 - z$; H) $-2 - x, -y, -z$.

There are two unique L^{3-} ligands in compound **5**, both of which are hexadentate and bridge six lead(II) ions through three phosphonate oxygen atoms and one sulfonate oxygen atom. Four phosphonate oxygen atoms [O(1), O(3), O(11), and O(12)] act as a μ^2-bridging ligand. A similar type of coordination mode has also been observed in compound **1**. Interconnection of the Pb^{II} ions through the bridging phosphonate groups leads to a 1D chain based on Pb_3O_4 cluster units (Figure 12, a). In contrast to the 1D chain in compound **1**, neighboring Pb_3O_4 cluster units within the chain are interconnected solely by the bridging phosphonate groups. These 1D chains are further cross-linked by the bridging L^{3-} and 4,4′-bipy ligands into a 3D network with small apertures along the *a*-axis (Figure 12,

b). Although fewer sulfonate oxygen atoms are involved in metal coordination in compound **5** than in compound **1**, the framework of compound **5** is still somewhat similar to that in compound **1**. The replacement of one aqua ligand in compound **1** by a nitrogen atom from a 4,4′-bipy ligand in compound **5** results in the splitting of the large cavities in compound **1** into two smaller parts (Figure 12). Due to the occupation of the cavities by the 4,4′-bipy ligands, compound **5** contains only a few lattice water molecules. A number of hydrogen bonds are formed among non-coordinating sulfonate oxygen atoms [O(7), O(9)], aqua ligands, and lattice water molecules (Table 1), with O···O contacts ranging from 2.84(2) to 2.93(1) Å.

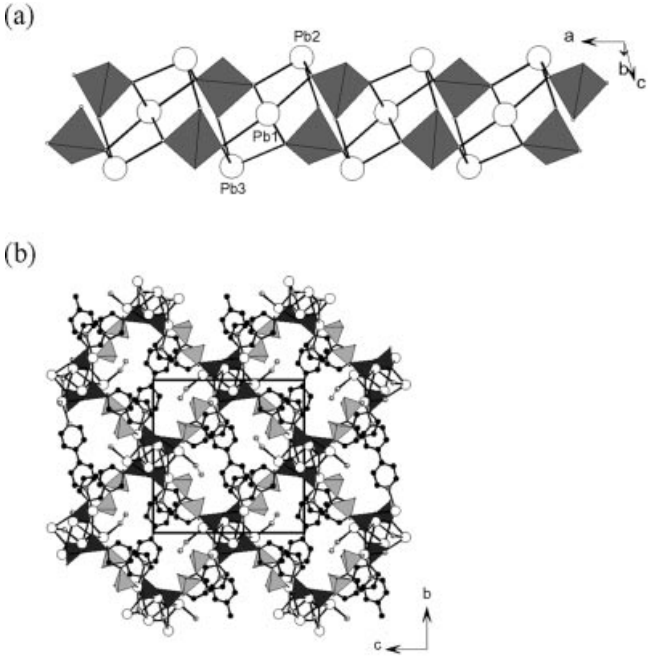

Figure 12. A 1D lead(II) phosphonate chain based on Pb_3O_4 units (a) and a view of the structure of compound **5** along the *a*-axis (b). The CPO_3 and CSO_3 groups are shaded in dark and medium grey, respectively. Pb, O, N, and C atoms are drawn as white, crossed, octanded, and black circles, respectively.

Luminescent Properties

The solid-state luminescent properties of compounds **1**, **2**, **3**, and **5** as well as the free phosphonate ligand were investigated at room temperature. The free ligand exhibits only a fluorescent emission band at λ_{max} = 370 nm upon excitation at 308 nm. The phen ligand displays a fluorescent emission band at λ_{max} = 381 nm with a shoulder at 364 nm upon excitation at 339 nm. Compound **1** displays a strong fluorescent emission band at λ_{max} = 398 nm (λ_{ex} = 330 nm; Figure 13) upon complexion of the L^{3-} ligands with the Pb^{II} ions, whereas compounds **2** and **3** display a weak broad emission band in the range 350–600 nm upon complexion of both sulfonate-phosphonate and phen ligands with the lead(II) ions. The bipy ligand displays a broad fluorescent emission band at λ_{max} = 423 nm (λ_{ex} = 345 nm), and upon complexion of both L^{3-} and bipy ligands with the Pb^{II} ions compound **5** displays a fluorescent emission band at λ_{max} = 420 nm (λ_{ex} = 330 nm; Figure 13). These emission bands are neither metal-to-ligand charge transfer (MLCT) nor ligand-to-metal charge transfer (LMCT) in nature, but rather can be attributed to an intraligand emission state.

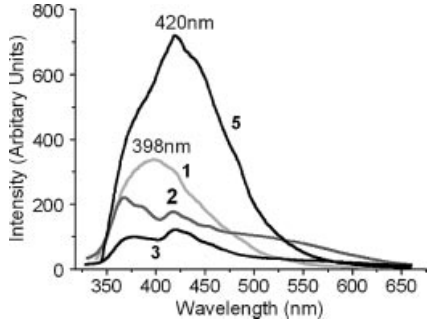

Figure 13. Solid-state emission spectra of compounds **1**, **2**, **3**, and **5**.

TGA Studies

The TGA curves of compounds **1**, **2**, **3**, and **5** all exhibit three main weight loss steps (Figure 14). The onset and final temperatures of these three steps as well as the weight

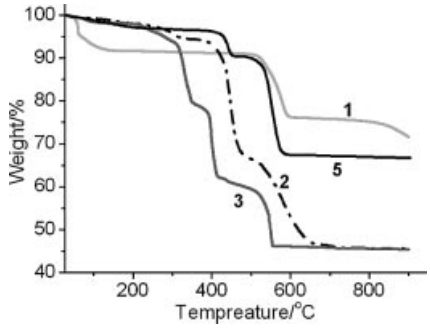

Figure 14. TGA curves for compounds **1**, **2**, **3**, and **5**.

Table 2. TGA data of compounds **1**, **2**, **3**, and **5**.

	First step		Second step	Third step	Total weight loss
	Temperature (onset/end) [°C]	Weight loss of H_2O (exp./calcd.) [%]	Temperature (onset/end) [°C]	Temperature (onset/end) [°C]	[%]
1	40/180	8.6/9.0	492/605	780/>900	28.4
2	45/205	2.5/2.8	240/336	370/735	54.1
3	40/115	1.7/1.5	182/415	415/556	54.6
5	40/209	2.9/3.0	360/455	486/600	32.6

losses are given in Table 2, where it can be seen that the observed weight losses of water molecules are close to the calculated values. The final residues were not characterized. The thermal stability of compound **4** was not studied due to our failure to obtain it as a single-phase product.

Conclusions

In summary, we have reported the hydrothermal synthesis, crystal structures, and characterization of five new lead(II) sulfonate-phosphonates, namely $[Pb_3(L)_2(H_2O)_2]\cdot 4H_2O$ (**1**), $[Pb(HL)(phen)]\cdot H_2O$ (**2**), $[Pb_6(L)_4(phen)_8]\cdot 3H_2O$ (**3**), $[Pb_6(L)_4(phen)_{10}]\cdot 2H_2O$ (**4**), and $[Pb_6(L)_4(4,4'\text{-bipy})(H_2O)_2]\cdot 2H_2O$ (**5**; H_3L = *m*-HO_3S-C_6H_4-PO_3H_2). The diverse structural frameworks of these five compounds depend on the flexible coordination ability of Pb^{II} as well as the mediation of an auxiliary ligand such as phen or 4,4′-bipy. *m*-Sulfophenylphosphonic acid is a versatile ligand that can adopt various coordination modes. In the absence of the second ligand or with 4,4′-bipy, which usually binds in a bidentate bridging mode, two types of 3D networks (compounds **1** and **5**) are obtained. The dimensionality of the structure is reduced when the bidentate chelating ligand phen is added as the second metal linker. Compound **2**, which has a layered structure, is obtained with a Pb/phen ratio close to 1:1. Further increase of the amount of phen and the pH leads to two types of discrete clusters (compounds **3** and **4**) which have the same skeleton but differ in the coordination numbers of the lead(II) ions. The results of our study indicate that by using *m*-sulfophenylphosphonic acid with phen as the auxiliary ligand we should be able to synthesize cluster compounds of not only d-block and f-block metals but also main group metals. Future research effects will be devoted to the designing of new types of cluster compounds containing other metal phosphonates.

Experimental Section

Materials and Methods: *m*-Sulfophenylphosphonic acid (*m*-HO_3S-C_6H_4-PO_3H_2, H_3L) was synthesized according to the procedures previously described by Montoneri.[14] All other chemicals were obtained from commercial sources and used without further purification. Elemental analyses were performed with an Elementary Vario EL III instrument. The FT-IR spectra were recorded with a Nicolet Magna 750 FT-IR spectrometer using KBr pellets in the range of 4000–400 cm^{-1}. Photoluminescence analyses were performed with a Perkin–Elmer LS55 fluorescence spectrometer. Thermogravimetric analyses were carried out with a NETZSCH STA 449C unit at a heating rate of 10 °C min^{-1} under an oxygen atmosphere. X-ray powder diffraction (XRD) patterns (Cu-K_α) were collected with a XPERT-MPD θ–2θ diffractometer.

Synthesis of $[Pb_3(L)_2(H_2O)_2]\cdot 4H_2O$ (1): The pH of a mixture of $Pb(OAc)_2$ (0.32 mmol) and H_3L (0.3 mmol) in 10 mL of distilled water was adjusted to about 4.8 with 1 M NaOH solution and the mixture was then sealed into a Parr Teflon-lined autoclave (23 mL) and heated at 150 °C for 4 d. The final pH was 4.6. Colorless brick-shaped crystals of **1** were collected in approx. 62% yield (0.079 g) based on Pb. The purity of this compound was confirmed by powder XRD (see Supporting Information). $C_{12}H_{20}O_{18}P_2S_2Pb_3$ (1199.9): calcd. C 12.01, H 1.68; found C 11.95, H 1.57. IR (KBr): $\tilde{\nu}$ = 3436 (s), 3059 (m), 2924 (m), 2852 (w), 1631 (m), 1402 (m), 1102 (s), 1022 (vs), 995 (vs), 962 (s), 800 (m), 669 (m), 618 (m), 557 (s) cm^{-1}.

Synthesis of $[Pb(HL)(phen)]\cdot H_2O$ (2): A mixture of $Pb(OAc)_2$ (0.3 mmol), H_3L (0.3 mmol), and phen (0.32 mmol) in 10 mL of distilled water, with an initial pH of 3.6, was sealed into a Parr Teflon-lined autoclave (23 mL) and heated at 150 °C for 4 d. The final pH remained unchanged. Colorless pillar-shaped crystals of **2** were collected in approx. 85% yield (0.16 g) based on Pb. The purity of this compound was confirmed by powder XRD (see Supporting Information). $C_{18}H_{15}N_2O_7PPbS$ (641.54): calcd. C 33.70, H 2.36, N 4.37; found C 33.75, H 2.68, N 4.29. IR (KBr): $\tilde{\nu}$ = 3582 (m), 3423 (m), 3062 (m), 2833 (m), 1624 (m), 1593 (m), 1520 (m), 1495 (m), 1428 (m), 1400 (m), 1188 (s), 1147 (s), 1106 (vs), 1025 (vs), 915 (s), 850 (s), 803 (m), 792 (m), 727 (m), 694 (m), 681 (m), 617 (m), 555 (s), 528 (m) cm^{-1}.

Synthesis of $[Pb_6(L)_4(phen)_8]\cdot 3H_2O$ (3): A mixture of $Pb(OAc)_2$ (0.36 mmol), H_3L (0.3 mmol), and phen (0.48 mmol) in 10 mL of distilled water, with its pH adjusted to about 4.0 with 1 M NaOH solution, was sealed into a Parr Teflon-lined autoclave (23 mL) and heated at 150 °C for 4 d. The final pH was 3.9. Colorless brick-shaped crystals of **3** were collected in approx. 77% yield (0.17 g) based on Pb. The purity of this compound was confirmed by powder XRD (see Supporting Information). $C_{120}H_{86}N_{16}O_{27}P_4Pb_6S_4$ (3679.3): calcd. C 39.17, H 2.36, N 6.09; found C 39.01, H 2.49, N 5.91. IR data (KBr): $\tilde{\nu}$ = 3435 (s), 3055 (m), 2923 (m), 2852 (m), 1621 (m), 1588 (m), 1512 (m), 1424 (m), 1343 (m), 1189 (s), 1097 (vs), 1029 (vs), 996 (s), 956 (m), 845 (m), 795 (m), 728 (m), 700 (m), 686 (m), 617 (m), 549 (m) cm^{-1}.

Synthesis of $[Pb_6(L)_4(Phen)_{10}]\cdot 2H_2O$ (4): A mixture of $Pb(OAc)_2$ (0.3 mmol), H_3L (0.27 mmol), and phen (0.5 mmol) in 10 mL of distilled water, with its pH adjusted to about 6.0 with 1 M NaOH solution, was sealed into a Parr Teflon™-lined autoclave (23 mL) and heated at 150 °C for 4 d. The final pH was 5.8. Colorless crystals of compound **4** were collected with some unidentified impurities. Although many experiments were performed under different reaction conditions, compound **4** could not be obtained as a single phase.

Synthesis of $[Pb_6(L)_4(4,4'\text{-Bipy})(H_2O)_2]\cdot 2H_2O$ (5): A mixture of $Pb(OAc)_2$ (0.36 mmol), H_3L (0.3 mmol), and 4,4′-bipy (0.25 mmol) in 10 mL of distilled water, with its pH adjusted to about 4.6 with 1 M NaOH solution, was sealed into a Parr Teflon-lined autoclave (23 mL) and heated at 150 °C for 4 d. The final pH was 4.7. Colorless brick-shaped crystals of **5** were collected in apprx. 64% yield (0.093 g) based on Pb. The purity of this compound was confirmed by powder XRD (see Supporting Information). $C_{34}H_{32}N_2O_{28}P_4Pb_6S_4$ (2411.9): calcd. C 16.93, H 1.34, N 1.16; found C 16.62, H 1.47, N 1.10. IR (KBr): 3435 (s), 3053 (m), 2924 (m), 2846 (w), 1604 (m), 1400 (m), 1220 (s), 1165 (s), 1101 (vs), 1059 (s), 1019 (vs), 995 (vs), 967 (vs), 796 (m), 686 (m), 623 (m), 552 (s) cm^{-1}.

Single-Crystal Structure Determination: Data collection for compounds **1**, **2**, and **5** was performed with a Siemens Smart CCD diffractometer, data collection for compound **3** was performed with a Mercury CCD diffractometer, and that for compound **4** with a Saturn 70 CCD diffractometer. All diffractometers were equipped with a graphite-monochromated Mo-K_α radiation source (λ = 0.71073 Å). Intensity data for all compounds were collected by the narrow frame method at 293 K. The data sets were corrected for Lorentz and polarization factors as well as for absorption with SADABS or by the multi-scan method.[15a,15b] All structures were

Table 3. Summary of crystal data and structural refinements for **1**–**5**.

	1	**2**	**3**	**4**	**5**
Empirical formula	$C_{12}H_{20}O_{18}P_2S_2Pb_3$	$C_{18}H_{15}N_2O_7PPbS$	$C_{120}H_{86}N_{16}O_{27}P_4S_4Pb_6$	$C_{144}H_{100}N_{20}O_{26}P_4S_4Pb_6$	$C_{34}H_{32}N_2O_{28}P_4S_4Pb_6$
Formula weight	1199.91	641.54	3679.30	4021.70	2411.88
Space group	$P2_1/n$	$P\bar{1}$	$P\bar{1}$	$P\bar{1}$	$P2_1/n$
a [Å]	10.3642(1)	7.2187(2)	14.963(4)	14.790(6)	10.2544(1)
b [Å]	15.5661(3)	11.0945(3)	15.141(4)	15.479(6)	16.3825(2)
c [Å]	16.4630(2)	11.7759(3)	15.471(4)	19.444(7)	16.6409(3)
α [°]	90.00	89.527(1)	68.069(7)	97.196(2)	90.000
β [°]	102.965(1)	78.516(1)	81.46(1)	106.154(2)	103.783(1)
γ [°]	90.00	84.841(1)	77.416(9)	111.849(4)	90.000
V [Å^3]	2588.27(6)	920.44(4)	3165(2)	3835(2)	2715.05(6)
Z	4	2	1	1	2
$D_{calcd.}$ [g cm^{-3}]	3.079	2.315	1.931	1.741	2.950
μ [mm^{-1}]	19.831	9.414	8.146	6.730	18.897
GOF on F_2	1.142	1.195	0.995	0.999	1.158
R_1,[a] wR_2[b] [$I > 2\sigma(I)$]	0.0264, 0.0524	0.0345, 0.0749	0.0493, 0.1255	0.0534, 0.1425	0.0357, 0.0666
R_1,[a] wR_2[b] (all data)	0.0368, 0.0558	0.0388, 0.0782	0.0766, 0.1436	0.0760, 0.1612	0.0484, 0.0711

[a] $R_1 = \Sigma||F_o| - |F_c||/\Sigma|F_o|$. [b] $wR_2 = \{\Sigma w[(F_o)^2 - (F_c)^2]^2/\Sigma w[(F_o)^2]^2\}^{1/2}$.

solved by direct methods and refined by full-matrix least-squares fitting on F^2 with SHELX-97.[15c] All non-hydrogen atoms, except O(2w) in compound **3**, were refined with anisotropic thermal parameters. All hydrogen atoms were generated geometrically and refined isotropically. The hydrogen atoms for the water molecules are not included in the refinements. Pb(3) in compound **3** is severely disordered and displays two orientations with 50% occupancy for each site. One sulfonate group in compound **2** is also severely disordered with O(11) exhibiting two orientations with 50% occupancy each. The occupancy factor of O(2w) in compound **3** was reduced to 50% due to its large thermal parameter. Important bond lengths are listed in Table 1. Crystallographic data and structural refinements for compounds **1**–**5** are summarized in Table 3.

CCDC-632076–632080 (for **1**–**5**) contain the supplementary crystallographic data for this paper. These data can be obtained free of charge from The Cambridge Crystallographic Data Center via www.ccdc.cam.ac.uk/data_request/cif.

Supporting Information (see also the footnote on the first page of this article): Figure S1. Simulated and experimental XRD powder patterns for compounds **1**, **2**, **3**, and **5** (Figure S1).

Acknowledgments

This work is supported by the National Natural Science Foundation of China (20521101), a Key Project of the Chinese Academy of Sciences (KJCX2-YW-H01), and the Natural Science Foundation of Fujian Province (E0420003, E0610034).

[1] a) A. Clearfield, *Metal Phosphonate Chemistry* in *Progress in Inorganic Chemistry* (Ed.: K. D. Karlin), John Wiley & Sons, New York, **1998**, vol. 47, pp. 371–510 and references cited therein; b) K. Maeda, *Microporous Mesoporous Mater.* **2004**, *73*, 47 and references cited therein; c) G. Nonglaton, I. O. Benitez, I. Guisle, M. Pipelier, J. Leger, D. Dubreuil, C. Tellier, D. R. Talham, B. Bujoli, *J. Am. Chem. Soc.* **2004**, *126*, 1497–1502; d) T. L. Schull, L. Henley, J. R. Deschamps, R. J. Butcher, D. P. Maher, C. A. Klug, K. Swider-Lyons, W. J. Dressick, B. Bujoli, A. E. Greenwood, L. K. B. Congiardo, D. A. Knight, *Organometallics* **2007**, *26*, 2272–2276.

[2] a) A. K. Cheetham, G. Férey, T. Loiseau, *Angew. Chem. Int. Ed.* **1999**, *38*, 3269–3292; b) J. Zhu, X. Bu, P. Feng, G. D. Stucky, *J. Am. Chem. Soc.* **2000**, *122*, 11563–11564; c) F. Fredoueil, M. Evain, D. Massiot, M. Bujoli-Doeuff, P. Janvier, A. Clearfield, B. Bujoli, *J. Chem. Soc. Dalton Trans.* **2002**, 1508–1512; d) P. Rabu, P. Janvier, B. Bujoli, *J. Mater. Chem.* **1999**, *9*, 1323–1326; e) N. Stock, S. A. Frey, G. D. Stucky, A. K. Cheetham, *J. Chem. Soc. Dalton Trans.* **2000**, 4292–4296.

[3] a) S. J. Hartman, E. Todorov, C. Cruz, S. C. Sevov, *Chem. Commun.* **2000**, 1213–1214; b) J.-G. Mao, Z. Wang, A. Clearfield, *Inorg. Chem.* **2002**, *41*, 2334–2340; c) J.-G. Mao, Z. Wang, A. Clearfield, *Inorg. Chem.* **2002**, *41*, 3713–3720.

[4] a) P. Yin, L.-M. Zheng, S. Gao, X.-Q. Xin, *Chem. Commun.* **2001**, 2346–2347; b) L.-M. Zheng, S. Gao, H.-H. Song, S. Decurtins, A. J. Jacobson, X.-Q. Xin, *Chem. Mater.* **2002**, *14*, 3143–3147; c) L.-M. Zheng, P. Yin, X.-Q. Xin, *Inorg. Chem.* **2002**, *41*, 4084–4086.

[5] a) E. Burkholder, V. Golub, C. J. O'Connor, J. Zubieta, *Chem. Commun.* **2003**, 2128–2129; b) R. C. Finn, E. Burkholder, J. Zubieta, *Chem. Commun.* **2001**, 1852–1853; c) R. C. Finn, J. Zubieta, *Inorg. Chem.* **2001**, *40*, 2466–2467; d) R. C. Finn, E. Burkholder, J. Zubieta, *Inorg. Chem.* **2001**, *40*, 3745–3754.

[6] a) C. Lei, J.-G. Mao, Y.-Q. Sun, H.-Y. Zeng, A. Clearfield, *Inorg. Chem.* **2003**, *42*, 6157–6159; b) J.-L. Song, H.-H. Zhao, J.-G. Mao, K. R. Dunbar, *Chem. Mater.* **2004**, *16*, 1884–1889; c) B.-P. Yang, J.-G. Mao, *Inorg. Chem.* **2005**, *44*, 566–571; d) J.-L. Song, J.-G. Mao, *Chem. Eur. J.* **2005**, *11*, 1417–1424; e) J.-L. Song, C. Lei, J.-G. Mao, *Inorg. Chem.* **2004**, *43*, 5630–5634.

[7] a) D. M. Poojary, B. Zhang, A. Cabeza, M. A. G. Aranda, S. Bruque, A. Clearfield, *J. Mater. Chem.* **1996**, *6*, 639–644; b) J.-G. Mao, Z. Wang, A. Clearfield, *Inorg. Chem.* **2002**, *41*, 6106–6111; c) J.-G. Mao, Z. Wang, A. Clearfield, *J. Chem. Soc. Dalton Trans.* **2002**, 4541–4546; d) M. M. Gomez-Alcantara, A. Cabeza, M. A. G. Aranda, A. Guagliardi, J.-G. Mao, A. Clearfield, *Solid State Sci.* **2004**, *6*, 479–487.

[8] a) S. Ayyappan, G. D. Delgado, A. K. Cheetham, G. Ferey, C. N. R. Rao, *J. Chem. Soc. Dalton Trans.* **1999**, 2905–2907; b) N. Stock, *Solid State Sci.* **2002**, *4*, 1089–1094; c) D. T. Tran, Y. S. Kam, P. Y. Zavalij, S. R. J. Oliver, *Inorg. Chem.* **2003**, *42*, 2165–2172; d) E. Irran, T. Bein, N. Stock, *J. Solid State Chem.* **2003**, *173*, 293–298.

[9] a) Z.-M. Sun, J.-G. Mao, Y.-Q. Sun, H.-Y. Zeng, A. Clearfield, *New J. Chem.* **2003**, *27*, 1326–1330; b) B.-P. Yang, J.-G. Mao, Y.-Q. Sun, H.-H. Zhao, A. Clearfield, *Eur. J. Inorg. Chem.* **2003**, 4211–4217; c) S.-M. Ying, J.-G. Mao, B.-P. Yang, Z.-M. Sun, *Inorg. Chem. Commun.* **2003**, *6*, 1319–1322; d) B.-P. Yang, Z.-M. Sun, J.-G. Mao, *Inorg. Chim. Acta* **2004**, *357*, 1583–1588.

[10] a) J.-L. Song, J.-G. Mao, Y.-Q. Sun, H.-Y. Zeng, R. K. Kremer, A. Clearfield, *J. Solid State Chem.* **2004**, *177*, 633–641; b) C. Lei, J.-G. Mao, Y.-Q. Sun, *J. Solid State Chem.* **2004**, *177*,

2449–2455; c) J.-L. Song, J.-G. Mao, *J. Mol. Struct.* **2005**, *740*, 181–186.
[11] a) J.-L. Song, J.-G. Mao, Y.-Q. Sun, A. Clearfield, *Eur. J. Inorg. Chem.* **2003**, 4218–4226; b) S.-M. Ying, J.-G. Mao, *Eur. J. Inorg. Chem.* **2004**, 1270–1276; c) Z.-M. Sun, J.-G. Mao, B.-P. Yang, S.-M. Ying, *Solid State Sci.* **2004**, *6*, 295–300; d) J.-L. Song, C. Lei, Y.-Q. Sun, J.-G. Mao, *J. Solid State Chem.* **2004**, *177*, 2557–2564; e) S.-M. Ying, J.-G. Mao, *J. Mol. Struct.* **2005**, *748*, 63–70; f) Z.-Y. Du, S.-M. Ying, J.-G. Mao, *J. Mol. Struct.* **2006**, *788*, 218–223.
[12] a) Z.-Y. Du, H.-B. Xu, J.-G. Mao, *Inorg. Chem.* **2006**, *45*, 6424–6430; b) Z.-Y. Du, H.-B. Xu, J.-G. Mao, *Inorg. Chem.* **2006**, *45*, 9780–9788.
[13] A. L. Spek, *Platon: A Multi-purpose Crystallographic Tool*, Utrecht University, The Netherlands, **2001**.
[14] a) E. Montoneri, *Phosphorus Sulfur Silicon Relat. Elem.* **1991**, *55*, 201–204; b) E. Montoneri, M. C. Gallazzi, *J. Chem. Soc. Dalton Trans.* **1989**, 1819–1823.
[15] a) G. M. Sheldrick, *Program SADABS*, University of Göttingen, Germany, **1995**; b) CrystalClear, version 1.3.5 Rigaku Corp., Woodlands, TX, **1999**; c) G. M. Sheldrick, *SHELX-96 Program for Crystal Structure Determination*, University of Göttingen, Germany, **1996**.

Received: April 27, 2007
Published Online: August 7, 2007

